OPTIMIZED LIFTING SCHEMES BASED ON ENO STENCILS FOR IMAGE APPROXIMATION

Mounir Kaaniche, Basarab Mateï

L2TI-LIPN, Institut Galilée,
Université Paris 13, Sorbonne Paris Cité
99 avenue Jean-Baptiste Clément
93430 Villetaneuse, France

Sylvain Meignen *

LJK, University of Grenoble
51 rue des mathématiques
38041 Grenoble cedex 09

ABSTRACT

In this paper, we propose to improve the classical lifting-based wavelet transforms by defining three classes of pixels which will be predicted differently. More specifically, the proposed idea is inspired by the Essentially Non-Oscillatory (ENO) transform and consists in shifting the stencil used for prediction in order to reduce the error near image singularities. Moreover, the different filters associated with these classes will be optimized in order to design a multiresolution representation well adapted to image characteristics. Our simulations show that the resulting multiscale representation leads to much lower amplitudes of the detail coefficients and improves the linear approximation properties.

Index Terms— Adaptive wavelets, Lifting scheme, ENO prediction, filter optimization, image approximation

1. INTRODUCTION

An alternative to the classical filter bank approach for the computation of the discrete wavelet transform (DWT) is the *lifting scheme* (LS), initially introduced by Sweldens [1, 2]. Due to their many advantages, LS has been found to be an efficient tool for still image coding [3, 4]. A generic LS applied to one dimensional (1D) signal consists of three successive steps referred to as *split, predict* and *update*. In the first step, the input 1D signal $s_j(n)$ is partitioned into two disjoint subsets formed by the even $s_{0,j}(n) := s_j(2n)$ and odd samples $s_{1,j}(n) := s_j(2n-1)$, respectively. Then, the *prediction* step consists in estimating the even samples $s_{0,j}(n)$ from the neighboring odd ones $s_{1,j}(n)$ (or inversely). Thus, a prediction error, called a detail signal, is then computed as follows:

$$d_{j+1}(n) = s_{0,j}(n) - \mathbf{p}_j^\top \mathbf{s}_{1,j}(n) \tag{1}$$

where $\mathbf{p}_j$ is the prediction filter, $\mathbf{s}_{1,j}(n) = (s_{1,j}(n-k))_{k\in\mathcal{P}_j}$, and $\mathcal{P}_j$ represents the support of $\mathbf{p}_j$. When the signal is highly correlated, using an appropriate prediction operator yields a detail signal d_{j+1} which contains much less information than the original one. Finally, the *update* step generates a coarser approximation of the original signal by smoothing the odd samples using the detail coefficients:

$$s_{j+1}(n) = s_{1,j}(n) + \mathbf{u}_j^\top \mathbf{d}_{j+1}(n) \tag{2}$$

where $\mathbf{u}_j$ is the update vector, $\mathbf{d}_{j+1}(n) = (d_{j+1}(n-k))_{k\in\mathcal{U}_j}$, and $\mathcal{U}_j$ represents the support of $\mathbf{u}_j$.

A separable 2D lifting scheme (2D-LS) is often implemented on an image by successively applying 1D-LS to its rows and columns (or inversely). This leads to an approximation coefficients and three detail coefficients subspaces. Then, a multiscale representation of the image is derived by recursively applying these steps to the resulting approximation coefficients.

In addition to the LS-based image representation, various attempts have been made to improve the wavelets by designing nonlinear transforms. For instance, a multiresolution transform, called the Piecewise Polynomial Harmonic (PPH), has been developed in [5] to take into account the potential irregularity in the input data. Moreover, Harten *et al.* have proposed another transform , referred to as Essentially Non-Oscillatory (ENO), in order to increase the accuracy of the prediction step near the jumps or the singularities of the data [6]. It is important to note that this transform has been extensively used in image processing [7, 8].

Motivated by the advantages of the latter transform, we propose in this paper to incorporate the concept of ENO in a typical LS-based wavelet transform. More precisely, contrary to the classical LS structure where a symmetric prediction filter is used by taking the same number of neighboring pixels located on the left and right side of the pixel to be predicted, the improved structure involves three kinds of prediction filters based on the characteristics of the pixel to be predicted. Thus, three classes of pixels will be defined. Moreover, the prediction filter associated with each class will be optimized in order to design a multiscale decomposition well adapted to the contents of the images.

The remainder of this paper is organized as follows. In

*This author acknowledges the support of the french national research agency (ANR) under the grant ANR-13-BS03-0002-01

Section 2, the principle of the nonlinear ENO transform is recalled. Then, the improved lifting structure based on optimized ENO filters is described in Section 3. Finally, experimental results are given in Section 4 and some conclusions are drawn in Section 5.

2. IMPROVED LIFTING SCHEME BASED ON ENO PREDICTION FILTERS

The most popular examples of LS are the family of $(L, \tilde{L})$ wavelet transforms where L and $\tilde{L}$ represent the number of coefficients of the prediction and update vectors, respectively. When $(L, \tilde{L}) = (4, 2)$, Eqs. (1) and (2) are expressed as:

$$d_{j+1}(n) = s_{0,j}(n) - \Big(\frac{9}{16}(s_{1,j}(n) + s_{1,j}(n+1)) - \frac{1}{16}(s_{1,j}(n-1) + s_{1,j}(n+2))\Big) \quad (3)$$

$$s_{j+1}(n) = s_{1,j}(n) + \frac{1}{4}(d_{j+1}(n) + d_{j+1}(n-1)). \quad (4)$$

Note that, in such a case, the prediction filter for an arbitrary length L is obtained by means of polynomial interpolation. Indeed, for a fixed n, let us consider the set $\{s_{1,j}(n-k)\}_{-\frac{L}{2}+1 \leq k \leq \frac{L}{2}}$ and the polynomial P that interpolates these L values at abscissae $(n-k)$. Then, one can check that the prediction vector satisfies $\mathbf{p}_j^\top \mathbf{s}_{1,j}(n) = P(n + \frac{1}{2})$. In this case, the corresponding multiresolution representation is equivalent to the Deslaurier-Dubuc interpolatory wavelet transform [9, 10]. Regarding the properties of the interpolant as well as the smoothness of the limit of this iterative process, the reader is referred to [9, 10, 11].

It is worth noting here that most prediction based on centered stencil, like the (4,2) LS, can be written in the following general form [12]:

$$\mathbf{p}_j^\top \mathbf{s}_{1,j}(n) = \frac{1}{2}(s_{1,j}(n) + s_{1,j}(n+1)) + f(\Delta^2 s_{1,j}(n), \Delta^2 s_{1,j}(n+1)), \quad (5)$$

where f is a given function and Δ^2 is the second order finite difference. PPH nonlinear transform [5] follows the same writing with:

$$\begin{aligned} & f(\Delta^2 s_{1,j}(n), \Delta^2 s_{1,j}(n+1)) = \\ & -\frac{1}{16}(sgn(\Delta^2 s_{1,j}(n)) + sgn(\Delta^2 s_{1,j}(n+1))) \\ & \times |\frac{\Delta^2 s_{1,j}(n) + \Delta^2 s_{1,j}(n+1)}{2}| \\ & \times (1 - |\frac{\Delta^2 s_{1,j}(n) - \Delta^2 s_{1,j}(n+1)}{\Delta^2 s_{1,j}(n) + \Delta^2 s_{1,j}(n+1)}|^2). \end{aligned} \quad (6)$$

As mentioned before, ENO has also been found to be an efficient transform that aims to improve the prediction process around the jumps or the singularities of the input data. In this context, the prediction filter is defined using polynomial interpolation on shifted stencils which leads, when a 3-rd order polynomial is used, to three kinds of prediction filters:

- centered prediction

$$\mathbf{p}_{j,c}^\top \mathbf{s}_{1,j}(n) = -\tfrac{1}{16}s_{1,j}(n-1) + \tfrac{9}{16}s_{1,j}(n) + \tfrac{9}{16}s_{1,j}(n+1) - \tfrac{1}{16}s_{1,j}(n+2) \quad (7)$$

- left-shifted prediction

$$\mathbf{p}_{j,l}^\top \mathbf{s}_{1,j}(n) = \tfrac{1}{16}s_{1,j}(n-2) - \tfrac{5}{16}s_{1,j}(n-1) + \tfrac{15}{16}s_{1,j}(n) + \tfrac{5}{16}s_{1,j}(n+1) \quad (8)$$

- right-shifted prediction

$$\mathbf{p}_{j,r}^\top \mathbf{s}_{1,j} \quad (n) = \tfrac{5}{16}s_{1,j}(n) + \tfrac{15}{16}s_{1,j}(n+1) - \tfrac{5}{16}s_{1,j}(n+2) + \tfrac{1}{16}s_{1,j}(n+3). \quad (9)$$

In that framework, at each location n of the even pixels to be predicted $s_{0,j}(n)$, one has to choose between three candidate prediction filters. To this end, the retained cost functions are firstly determined from the neighboring odd samples as follows:

$$\begin{aligned} \Delta_{c,j}(n) &= |s_{1,j}(n+1) - s_{1,j}(n)|, \\ \Delta_{l,j}(n) &= |s_{1,j}(n) - s_{1,j}(n-1)|, \\ \Delta_{r,j}(n) &= |s_{1,j}(n+2) - s_{1,j}(n+1)|. \end{aligned}$$

After that, according to the obtained cost functions, three classes image labelling $\mathcal{L}_j(n)$ are deduced:

$$\text{If } \Delta_{l,j}(n) > \Delta_{c,j}(n) \text{ and } \Delta_{r,j}(n) > \Delta_{c,j}(n), \quad \mathcal{L}_j(n) = 0. \quad (10)$$

$$\text{If } \Delta_{c,j}(n) > \Delta_{l,j}(n) \text{ and } \Delta_{r,j}(n) > \Delta_{l,j}(n), \quad \mathcal{L}_j(n) = -1. \quad (11)$$

$$\text{If } \Delta_{c,j}(n) > \Delta_{r,j}(n) \text{ and } \Delta_{l,j}(n) > \Delta_{r,j}(n), \quad \mathcal{L}_j(n) = 1. \quad (12)$$

Finally, if $\mathcal{L}_j(n) = 0$ (resp. -1 or 1), the centered (resp. left or right shifted) prediction is used to predict the pixel $s_{0,j}(n)$ and generate the detail coefficients $d_{j+1}(n)$.

3. MULTISCALE REPRESENTATION USING OPTIMIZED ENO PREDICTION FILTERS

Once the modified LS structure based on the ENO prediction filters has been described, we now focus on the optimization task of the different possible predictors $\mathbf{p}_{j,c}$, $\mathbf{p}_{j,l}$ and $\mathbf{p}_{j,r}$.

3.1. Determination of the labels

To build the labels $\mathcal{L}_j(n)$ of the different resolution levels for an original input image S_0, we define S_J the image subsampled by a factor of 2^J and then compute the linear approximation of S_{J-1} using centered prediction on the columns and then on the rows without adding any detail coefficients. By iterating on this approximation $J-1$ times, we obtain an approximation of S_0. At each time, the labels $\mathcal{L}_j(n)$ are computed by using Eqs. (10)-(12). We should note here that, when the update step is omitted, such determination procedure allows to ensure that the labels are the same at the direct and inverse steps of the decomposition, and so, guarantees the stability of the transform. However, this property will not be satisfied when an update step is performed to compute the approximation coefficients.

3.2. Design of the optimized ENO prediction filters

Aiming at producing a multiscale decomposition well adapted to the image content, we propose here to optimize the ENO prediction filters by minimizing the variance of the prediction error (i.e. the detail signal). To this end, we recall that the detail coefficients are computed as follows:

$$d_{j+1}(n) = \begin{cases} s_{0,j}(n) - \mathbf{p}_{j,c}^{\top}\mathbf{s}_{1,j,c}(n) \ \text{ if } \mathcal{L}_j(n)=0 \\ s_{0,j}(n) - \mathbf{p}_{j,l}^{\top}\mathbf{s}_{1,j,l}(n) \ \text{ if } \mathcal{L}_j(n)=-1 \\ s_{0,j}(n) - \mathbf{p}_{j,r}^{\top}\mathbf{s}_{1,j,r}(n) \ \text{ if } \mathcal{L}_j(n)=1, \end{cases} \quad (13)$$

where $\mathbf{s}_{1,j,c}(n) = (s_{1,j}(n-1), s_{1,j}(n), s_{1,j}(n+1), s_{1,j}(n+2))^{\top}$, $\mathbf{s}_{1,j,l}(n) = \mathbf{s}_{1,j,c}(n-1)$ and $\mathbf{s}_{1,j,r}(n) = \mathbf{s}_{1,j,c}(n+1)$. By minimizing the variance of the detail coefficients, the optimal prediction vectors $\mathbf{p}_{j,c}^{\text{opt}}$, $\mathbf{p}_{j,l}^{\text{opt}}$ and $\mathbf{p}_{j,r}^{\text{opt}}$ can be determined by solving the Yule-Walker equations:

$$\mathbb{E}[\mathbf{s}_{1,j,c}(n)\mathbf{s}_{1,j,c}^{\top}(n)]\mathbf{p}_{j,c}^{\text{opt}} = \mathbb{E}[s_{0,j}(n)\mathbf{s}_{1,j,c}(n)] \ \text{ if } \mathcal{L}_j(n)=0 \quad (14)$$

$$\mathbb{E}[\mathbf{s}_{1,j,l}(n)\mathbf{s}_{1,j,l}^{\top}(n)]\mathbf{p}_{j,l}^{\text{opt}} = \mathbb{E}[s_{0,j}(n)\mathbf{s}_{1,j,l}(n)] \ \text{ if } \mathcal{L}_j(n)=-1 \quad (15)$$

$$\mathbb{E}[\mathbf{s}_{1,j,r}(n)\mathbf{s}_{1,j,r}^{\top}(n)]\mathbf{p}_{j,r}^{\text{opt}} = \mathbb{E}[s_{0,j}(n)\mathbf{s}_{1,j,r}(n)] \ \text{ if } \mathcal{L}_j(n)=1. \quad (16)$$

It should be noticed here that the optimization is performed on each class of pixels. Moreover, two strategies will be considered in this work. The first one is a global approach where the three optimized filters are firstly computed over all the rows of the image S_j in order to generate the approximation subband $S_{j+\frac{1}{2}}$ and the detail one $D_{j+\frac{1}{2}}$. After that, the same optimization procedure is applied along the columns of $S_{j+\frac{1}{2}}$ and $D_{j+\frac{1}{2}}$ to produce the approximation subband S_{j+1} as well as the three detail subbands. However, the second one is a local approach which consists in determining the optimal prediction filters for each row of the image and then for each column. Concerning the update step, and for the sake of simplicity, we have used for the different resolution levels the same update operator given by Eq. (4).

4. EXPERIMENTAL RESULTS

In this part, we study the ability of the different multiscale techniques to accurately represent an image without adding any new details. More precisely, we propose to construct an approximation of image S_0 of size $N \times M$ only knowing its approximation S_J for a certain resolution level $J \geq 1$. To this end, we consider the following transforms.
The first one, denoted by LS, is the classical LS-based wavelet transform defined by Eqs. (3). The second and the third ones are the nonlinear PPH [5] and ENO transforms [12]. Finally, the improved lifting scheme based on the optimized ENO prediction filters is designated by LS-ENO-OPT-L (resp. LS-ENO-OPT-G) where a local (resp. global) optimization approach is considered. To show the interest of the proposed transforms, we also compare them with the optimized version of the classical LS-based wavelet transform which will be denoted by LS-OPT-L and LS-OPT-G. Note that the latter, where only the centered prediction is considered and then optimized, has already been studied in the literature [13, 14].

4.1. Image reconstruction using approximation subspace

First, Figures 1(a) and 1(b) illustrate the PSNR of the reconstructed images with respect to the proportion of coefficients kept for images "Einst" and "Cameraman", respectively. Note that one half (resp. fourth) of the coefficients are kept when the approximation of S_0 is built from $S_{\frac{1}{2}}$ (resp. S_1). Let us recall that the PSNR is given by:

$$\text{PNSR} = 10\log_{10}\left(\frac{255^2}{\frac{1}{NM}\sum_{n,m}(S_0(n,m) - \hat{S}_0(n,m))^2}\right), \quad (17)$$

where $\hat{S}_0$ stands for the linear approximation of S_0.
Thus, it can be noticed that using either nonlinear prediction filters such as PPH prediction, keeping a centered stencil as performed in the classical LS, or optimizing the filters globally leads to similar or small improvement of the quality of the linear approximation compared with the fixed linear techniques based on LS. Moreover, our improved LS based on ENO prediction filters, optimized through a local approach, yields the best linear approximation results. Such results confirm that the three retained classes are really discriminant and give rise to different optimal predictors.

4.2. Decay of detail coefficients

In addition, the quality of approximation given by the different multiscale representations is also measured by the decay of the detail coefficients: the faster the coefficients decay, the more compact the representation. Fig. 2(a) (resp. 2(b)) displays the detail coefficients ranked in decreasing order when one (resp. two) resolution levels of decomposition is considered. The obtained results show that LS-ENO-OPT-L yields detail coefficients that decay much faster than those obtained

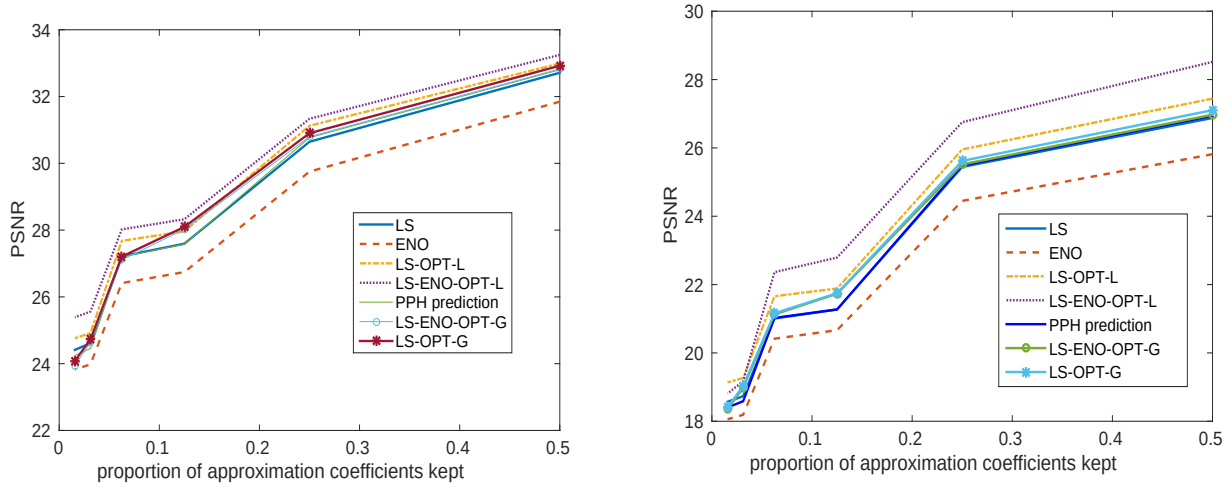

(a) (b)

Fig. 1. Linear approximation results using only a certain approximation subspace for the images: (a) Einst, (b) Cameraman

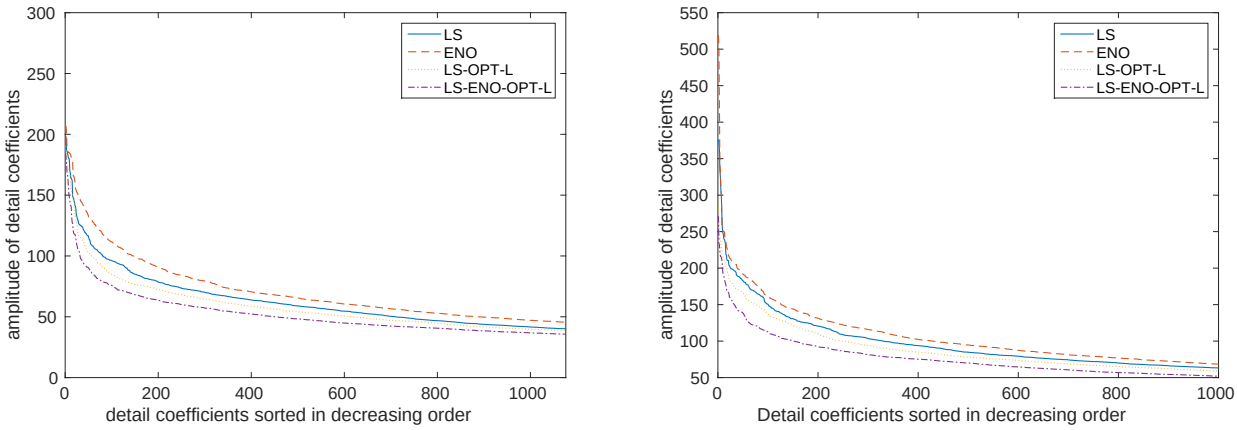

(a) (b)

Fig. 2. Decay of detail coefficients associated with: (a) one level of decomposition, (b) two levels.

with the other transforms, which confirm again the interest of the proposed multiresolution representation.

5. CONCLUSION AND PERSPECTIVES

In this paper, we have presented an improved LS-based wavelet transform based on ENO prediction filters. The optimization of these operators over three classes of pixels has also been investigated. Experimental results have shown the benefits of the resulting multiscale decomposition in terms of quality of approximation. Since the optimized filters are determined based on a local approach, this requires to efficiently store the filter coefficients. This constitutes a first issue that will be addressed in a future work. Moreover, due to its interesting linear approximation properties, we propose also to investigate this kind of representation to design an efficient image coding scheme.

6. REFERENCES

[1] W. Sweldens, "The lifting scheme: A custom-design construction of biorthogonal wavelets," *Applied and Computational Harmonic Analysis*, vol. 3, pp. 186–200, April 1996.

[2] R. L. Claypoole, G. M. Davis, W. Sweldens, and R. G. Baraniuk, "Nonlinear wavelet transforms for image cod-

ing via lifting," *IEEE Transactions on Image Processing*, vol. 12, no. 12, pp. 1449–1459, December 2003.

[3] D. Taubman and M. Marcellin, *JPEG2000: Image Compression Fundamentals, Standards and Practice*, Kluwer Academic Publishers, Norwell, MA, USA, 2001.

[4] M. Kaaniche, B. Pesquet-Popescu, A. Benazza-Benyahia, and J.-C. Pesquet, "Adaptive lifting scheme with sparse criteria for image coding," *EURASIP Journal on Advances in Signal Processing: Special Issue on New Image and Video Representations Based on Sparsity*, vol. 2012, 22 pages, January 2012.

[5] S. Amat and J. Liandrat, "On the stability of the pph nonlinear multiresolution," *Applied and computational harmonic analysis*, vol. 18, pp. 198–206, March 2005.

[6] A. Harten, B. Enquist, S. Osher, and S. Chakravarthy, "Uniformly high order accurate essentially non-oscillatory schemes III," *Journal of Computational Physics*, vol. 131, pp. 3–47, February 1997.

[7] S. Amat, F. Arandiga, A. Cohen, R.Donat, G.Garcia, and M.Von Oehsen, "Data compression with ENO schemes - a case study," *Applied and Computational Harmonic Analysis*, vol. 11, no. 12, pp. 273–288, September 2001.

[8] F. Arandiga, A. Cohen, R. Donat, N. Dyn, and B. Matei, "Approximation of piecewise smooth images by edge-adapted techniques," *Applied and Computational Harmonic Analysis*, vol. 24, pp. 225–250, March 2008.

[9] G. Deslaurier and S. Dubuc, "Symmetric iterative interpolation scheme," *Constructive Approximation*, vol. 5, pp. 49–68, January 1989.

[10] N. Dyn, J. Gregory, and D. Levin, "Analysis of uniform binary subdivision schemes for curve design," *Constructive Approximation*, vol. 7, pp. 127–147, January 1991.

[11] I. Daubechies and J. Lagarias, "Two scale differences equations: I.existence and global regularity of solutions," *SIAM J. Math. Anal.*, vol. 22, pp. 1388–1410, September 1991.

[12] B. Matei and S. Meignen, "Analysis of a class of nonlinear and non-separable multiscale representations," *Numerical Algorithms*, vol. 60, pp. 391–418, July 2012.

[13] M. Kaaniche, A. Benazza-Benyahia, B. Pesquet-Popescu, and J-C. Pesquet, "Non-separable lifting scheme with adaptive update step for still and stereo image coding," *Signal Processing*, vol. 91, pp. 2767–2782, December 2011.

[14] G. Piella, B. Pesquet-Popescu, H. Heijmans, and G. Pau, "Combining seminorms in adaptive lifting schemes and applications to image analysis and compression," *Journal of Mathematical Imaging and Vision*, vol. 25, no. 2, July 2006.